

## INVESTIGATION OF SURFACE ROUGHNESS IMPACT ON MEAN WIND FLOW USING RNG $k-\epsilon$ MODEL

Sheikh Ahmad Zaki<sup>a\*</sup>, Ahmad Zaki Jaafar<sup>a</sup>, Ahmad Faiz Mohammad<sup>a</sup>, Mohamed Sukri Mat Ali<sup>a</sup>, Azli Abd Razak<sup>b</sup>

<sup>a</sup>Malaysia-Japan International Institute of Technology, Universiti Teknologi Malaysia, Kuala Lumpur, Malaysia

<sup>b</sup>Faculty of Mechanical Engineering, Universiti Teknologi MARA, Shah Alam, Malaysia

### Article history

Received

17 August 2015

Received in revised form

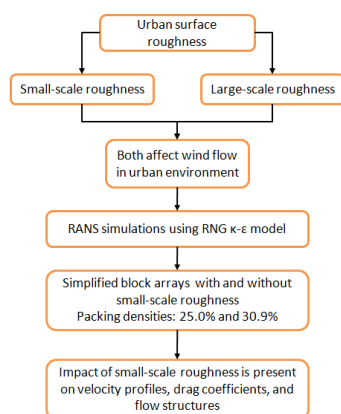
10 April 2015

Accepted

15 August 2015

\*Corresponding author  
sheikh.kl@utm.my

### Graphical abstract



### Abstract

Wind flow in the urban boundary layer is influenced by both large- and small-scale surface roughness. In this study, Reynolds-averaged Navier-Stokes simulations using the renormalisation group (RNG)  $k-\epsilon$  model were performed to study the wind flow in square arrays with small-scale roughness elements at the front and back of cubical obstacles at packing densities of 25.0% and 30.9%. The presence of small-scale roughness reduces streamwise velocity but increases turbulent kinetic energy. Moreover, small vortices are formed within the canopy because of small-scale roughness. The generated streamwise velocity profiles are similar at packing densities of 25.0% and 30.9%, but the drag coefficient is higher in the latter case. In brief, the impact of small-scale roughness on urban wind flow is considerable. The results of this study can contribute to future research on wind flow, particularly in the urban environment.

**Keywords:** Small-scale roughness, urban canopy flow, packing density, streamwise velocity, turbulent kinetic energy, renormalisation group  $k-\epsilon$  model

### Abstrak

Aliran angin dalam lapisan arus udara di kawasan bandar dipengaruhi oleh kekasaran permukaan yang secara asasnya terdiri daripada objek berskala besar dan kecil. Dalam kajian ini, simulasi "Reynolds-averaged Navier-Stokes menggunakan model *renormalisation group* (RNG)  $k-\epsilon$ " dijalankan untuk menyiasat keadaan aliran angin dalam kelompok bangunan yang terdiri daripada objek yang berskala kecil pada permukaan hadapan dan belakang blok yang dibina untuk kepadatan kawasan 25.0% dan 30.9%. Kehadiran objek berskala kecil itu mengurangkan halaju aliran angin tetapi meningkatkan tenaga kinetik turbulen. Tambahan, vorteks yang kecil dalam bahagian kanopi terbentuk akibat daripada objek berskala kecil itu. Untuk kepadatan 25.0% dan 30.9%, halaju aliran angin yang dihasilkan adalah sama dalam kedua-dua kes tetapi daya seretan adalah lebih tinggi untuk kes yang kedua. Secara kesimpulannya, kesan elemen objek berskala kecil terhadap aliran angin di kawasan bandar tidak boleh diabaikan. Hasil kajian ini penting untuk penyiasatan yang seterusnya terutamanya dalam kawasan persekitaran bandar.

**Kata kunci:** Kekasaran objek berskala kecil, aliran angin kanopi, kepadatan kawasan, aliran angin, tenaga kinetik turbulen, simulasi model *renormalisation group*  $k-\epsilon$

© 2016 Penerbit UTM Press. All rights reserved.

## 1.0 INTRODUCTION

The study of the wind characteristics of the urban canopy layer is important for understanding pollutant dispersion, improving air quality, and achieving thermal comfort, as human activities are conducted within this layer. Because urban areas contain various types of buildings that act as obstacles to wind, the wind flow pattern is complex. Turbulent flow results from the interaction between wind and building surfaces. A portion of the wind that infiltrates the urban geometry provides ventilation and removes pollutants [1]. Observations within the urban boundary layer focus on the complex interaction between usual flow conditions and various urban geometries and include mean flow patterns and turbulent kinetic energy (TKE) generated around the buildings.

The mean and turbulent wind velocities in the urban boundary layer are strongly influenced by surface roughness, which depends on the dimensions and positions of buildings. Oke [2] recognised that the pattern of air flow changes with respect to the aspect ratio, defined as the ratio of building height to the buildings' separation distance ( $H/W$ ). This pattern can be classified into three flow regimes, as shown in Figure 1 from Oke: isolated roughness flow ( $H/W < 0.7$ ), wake interference flow ( $0.4 < H/W < 0.7$ ), and skimming flow ( $H/W > 0.4$ ). Skimming flow typically occurs in cases of dense urban condition. Packing density ( $\lambda_p$ ) is a primary geometric parameter representing the denseness or sparseness of an urban area and is determined by the ratio of the surface area of the top of buildings (i.e. blocks in this study) to the total surface area. Therefore, a higher  $\lambda_p$  indicates close proximity of buildings to one another and likely generates wake interference flow and skimming flow between buildings.

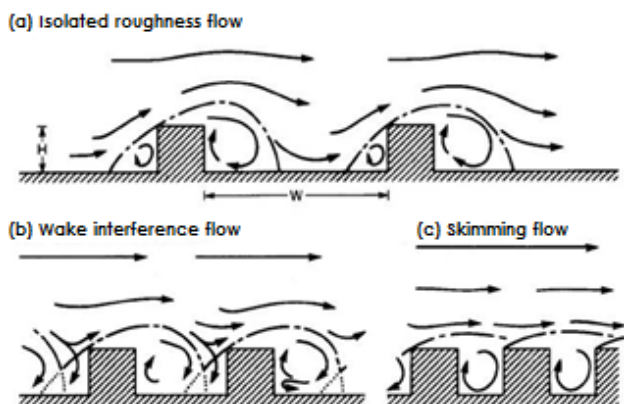


Figure 1 Pattern of air flow based on aspect ratio [2]

Many studies have used simplified urban models to investigate flow patterns and structures. Specifically, direct numerical simulation (DNS) has been used to simulate turbulent flow over regular arrays of cubical obstacles [3]. In addition, a set of systematic experiments was conducted to measure vertical

velocity profiles over a two-dimensional obstacle array, adding small-scale roughness elements to the top of large, parallel square bars [4]. Small-scale roughness elements exist in many forms, such as a chimney, roof, or extended part of a dwelling, in real urban environments.

In some parts of Malaysia, dwellings are commonly modified to extend living space and improve inhabitants' comfort [5, 6]. The modification effects on the wind environment in the surrounding area are not fully represented. Current literature lacks both quantitative and qualitative analysis on the small-scale roughness effect mainly on the mean flow field within the canopy layer. In fact, the flow regime and wind velocity are possibly affected by the presence of the small-scale roughness. Therefore, this study investigates the impact of small-scale roughness elements, i.e. additional structures on a main block, on the wind flow of a turbulent boundary layer over block arrays using Reynolds-averaged Navier-Stokes (RANS) simulations of the renormalisation group (RNG)  $k-\epsilon$  model.

## 2.0 MATERIALS AND METHODS

RANS simulations were conducted using the RNG  $k-\epsilon$  model with OpenFOAM® 2.3, an open-source software package. The application solves the Navier-Stokes equations that govern flow behaviour through iterative computation. The solution is produced by the discretisation method, which transforms physical processes and equations into discrete counterparts based on control-volume equations that generate finite volumes.

Two types of blocks were used in this study, as shown in Figure 2. The first was a cubical block with 25-mm edges (representing large-scale roughness). The second was the same cubical block with small-scale roughness in the form of rectangular blocks attached to its front and back sides. The dimensions of the rectangular blocks were  $25 \times 6.25 \times 6.25$  mm.

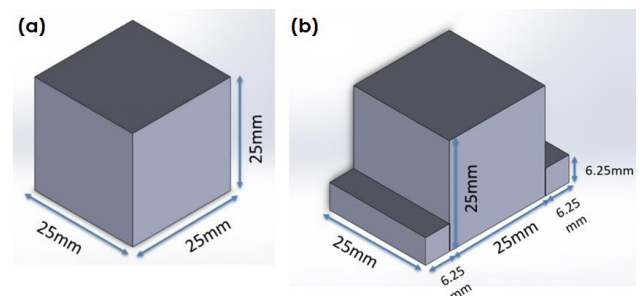
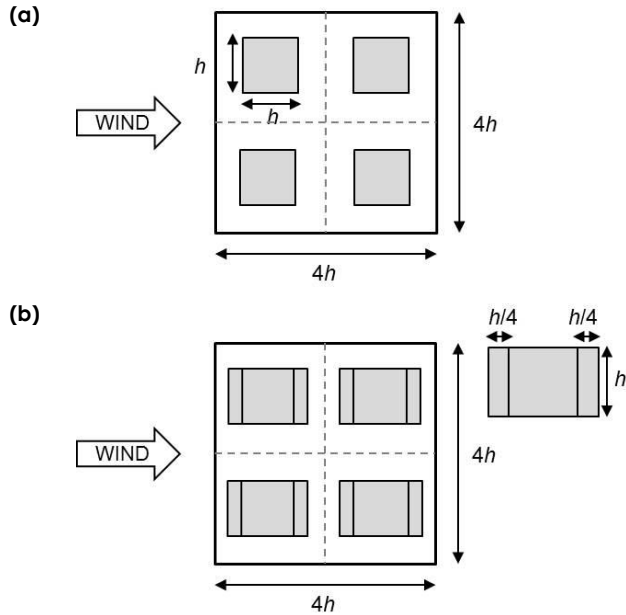


Figure 2 Types of blocks: (a) cubical block and (b) cubical block with small-scale roughness

Based on these two types of blocks, two primary simulation cases were designed. Case A consisted of only four cubical blocks, while case B consisted of four cubical blocks with small-scale roughness. Each

case was tested for two packing densities, 25.0% and 30.9%. The schematic diagrams for both cases are shown in planar view in Figure 3. The height of the domain is  $4h$ , where  $h$  is the block height (25 mm).  $4h$  was deduced sufficient [3] to capture the influence of roughness within the canopy layer.



**Figure 3** Simulation cases in planar view: (a) case A, cubical block array and (b) case B, cubical block array with small-scale roughness

The flow in the internal domain was driven by a pressure gradient defined as follows:

$$\frac{\partial P}{\partial x} = -\frac{\rho U_*^2}{L_z}, \quad (1)$$

The boundary conditions for both cases are shown in Figure 4. A cyclic condition was imposed in the streamwise direction and on the lateral boundaries to create an infinite domain [3, 7]. A free-slip condition for velocity and pressure was imposed on the top boundary. A no-slip condition (zero initial pressure and velocity) and wall functions were applied to the surfaces of the blocks and the floor. The wall functions (kqRWallFunction for turbulent kinetic energy or  $\kappa$  and epsilonWallFunction for dissipation rate of turbulent kinetic energy or  $\epsilon$ ) are based on logarithmic wind profile. It was applied primarily to optimize the use of computational resources without opting for higher grid refinements which might have been time-consuming.

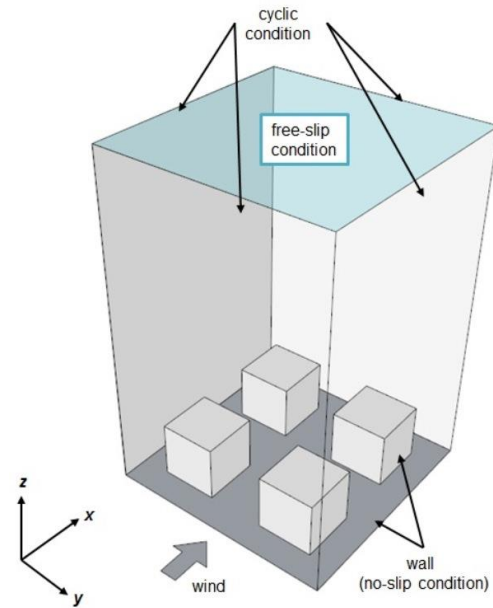


**Figure 4** Boundary conditions of the domain for the simulations

The physical properties of air are based on sea-level conditions, including air density ( $\rho = 1.225 \text{ kg/m}^3$ ) and kinematic viscosity ( $\nu = 1.046 \times 10^{-5} \text{ m}^2/\text{s}$ ). Reynolds number,  $Re$ , is calculated using Equation 2.1, as follows:

$$Re = U \times h / \nu, \quad (2)$$

where  $U$  is the reference streamwise velocity (7 m/s), and  $h$  is the height of the block (25 mm). The Reynolds number for both cases was 16,730, which is in the required range of 300 to 20,920 for Reynolds-number independence [8].

Grid refinement of  $h/16$  was chosen based on an analysis of previous numerical studies. For instance, the results for streamwise velocity profiles obtained for the grid distributions of  $h/16$  and  $h/25$  illustrated an insignificant level of discrepancy [9]. It was thus inferred that the grid distribution of  $h/16$  was sufficiently reliable for the study mainly because the analysis target was on mean flow properties. This choice also shortened the time needed for the simulation.

The pimpleFoam solver was used to compute the solution for incompressible flow. The PIMPLE algorithm is a combination of the Pressure Implicit Splitting of Operators (PISO) and Semi-Implicit Method for Pressure-Linked Equations (SIMPLE) algorithms. In the SIMPLE algorithm, a pressure-correction term is used, while the velocity corrections are ignored because they are unknown. The PISO algorithm performs a velocity correction after the first stage, leading to additional pressure corrections. In the solver settings, convergence was set to achieve when the scale residuals stabilized and reached a minimum of  $10^{-6}$  for velocity and  $10^{-5}$  for  $\kappa$  and  $\epsilon$ .

### 3.0 RESULTS AND DISCUSSION

#### 3.1 Streamwise Velocity Profiles

For validation purposes, streamwise velocity profiles of a square block array ( $\lambda_p = 25.0\%$ ) were plotted for three different studies (Figure 5), including the results from case A of this study, labelled as 'RANS'. The results from case B were not included in Figure 5 since the validation is focused on the results' accuracy, exclusive of the impact of small-scale roughness. Additionally, DNS refers to the DNS study by Coceal *et al.* [3], while LES refers to the large-eddy simulation (LES) study of Mohammad *et al.* [10]. The y-axis displays the elevation normalised by the cube height. The x-axis displays the normalised streamwise velocity,  $U_{mean}/U_h$ , where  $U_h$  is the spatially averaged velocity at the block height ( $z/h = 1$ ). From the figure, the RANS profile closely matches both the LES and DNS profiles in the region above the block height. From the floor surface to the canopy layer, however, the RANS profile deviates from the LES and DNS profiles. This can be attributed to the limitations of RANS in accurately capturing the potentially dominant turbulence in this region due to the stronger influence of wall surfaces (i.e. blocks and floor). Thus, the interaction between the flow and the surfaces is enhanced, resulting in greater surface drag in the canopy region [11, 12].

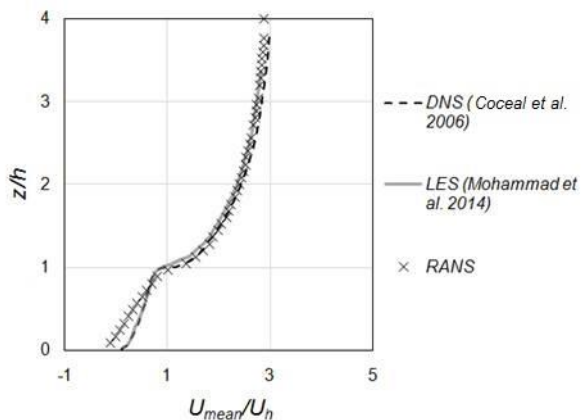


Figure 5 Mean streamwise velocity profiles

As shown in Figure 5, there is discrepancy in the results of the studies below the canopy layer because the DNS and LES solutions captured and solved eddies in the canyon, while the RANS solution simply averaged the unsteadiness of the flow [3, 10, 13]. As a result, the mean velocity below the block height in the RANS solution is lower than in the LES and DNS solutions. Generally, however, the RANS streamwise velocity profile is comparable to those of both LES and DNS, and the validation provides convincing results.

In addition, the streamwise velocity profiles of four RANS simulations in this study were plotted to

compare the results between cases A and B with two different packing densities:  $\lambda_p = 25.0\%$  and  $\lambda_p = 30.9\%$ .

Figure 6 shows the graph of  $z/h$  plotted against  $U_{mean}/U_h$ . Streamwise velocity increases with height in all cases. There is no discrepancy between cases A and B for 25.0% packing density. However, for 30.9% packing density, an obvious discrepancy lies within the canopy region near the floor surface ( $0 \leq z/h \leq 0.25$ ). The deviation of the profile of case B from that of case A can be attributed to the impact of wind velocity due to the presence of small-scale roughness.

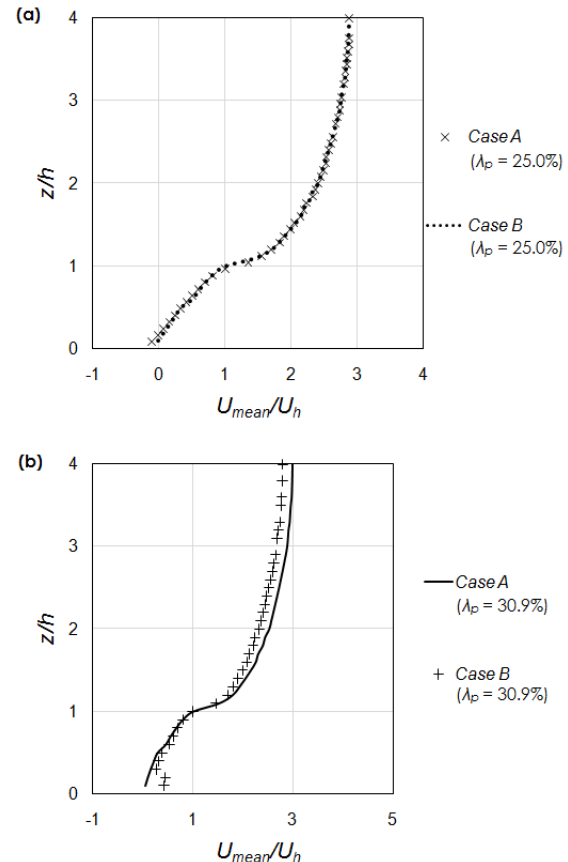
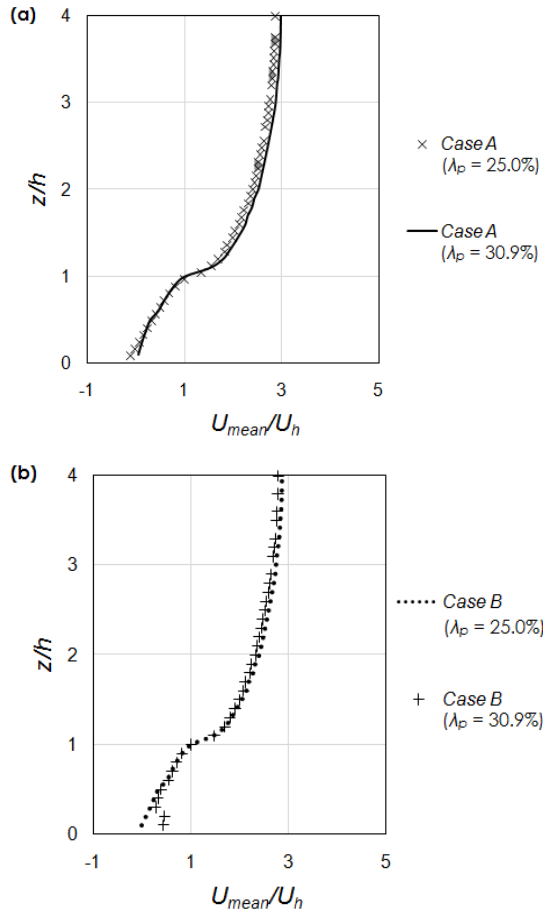


Figure 6 Comparison of velocity profiles of cases A and B with (a)  $\lambda_p = 25.0\%$  and (b)  $\lambda_p = 30.9\%$

Figure 7 provides further comparison of the effects of packing density. In Figure 7(a), the results of case A for  $\lambda_p = 25.0\%$  and  $\lambda_p = 30.9\%$  show similarity in the streamwise velocity profiles. Only a small difference between the two occurs near the ground level. This can be attributed to the surface shear of the floor, which tends to generate eddies and lead to discrepancies in the mean wind flow [3, 7]. In addition, Figure 7(b) shows a noticeable discrepancy between  $z/h$  values of 0 and 0.25, as mentioned previously. This finding indicates that the impact of small-scale roughness on streamwise velocity is more pronounced when blocks are in closer proximity to one another ( $\lambda_p = 30.9\%$ ). Therefore, it is possible that

in less dense block arrays ( $\lambda_p = 25.0\%$  or less), small-scale roughness may not substantially obstruct streamwise flow.



**Figure 7** Comparison of velocity profiles for  $\lambda_p = 25.0\%$  and  $\lambda_p = 30.9\%$  in (a) case A and (b) case B

### 3.2 Turbulent Kinetic Energy (TKE)

TKE is a measure of the amount of energy in turbulent flow. It can roughly represent the intensity of eddies in the mean flow or the propensity of the flow in generating vortices, which are related to TKE dissipation [14].

Figure 8 compares the mean TKE profiles for cases A and B, and Figure 9 compares those for 25.0% and 30.9% packing densities. Both figures show that TKE increases significantly from the ground level to the block height. Based on this profile, the highest TKE occurs slightly above the block height, and a decrease in mean TKE is observed from the canopy layer to the top of the domain. This decreasing pattern can be attributed to the stabilisation of the mean flow due to the reduced shear force caused by the underlying blocks [3, 15].

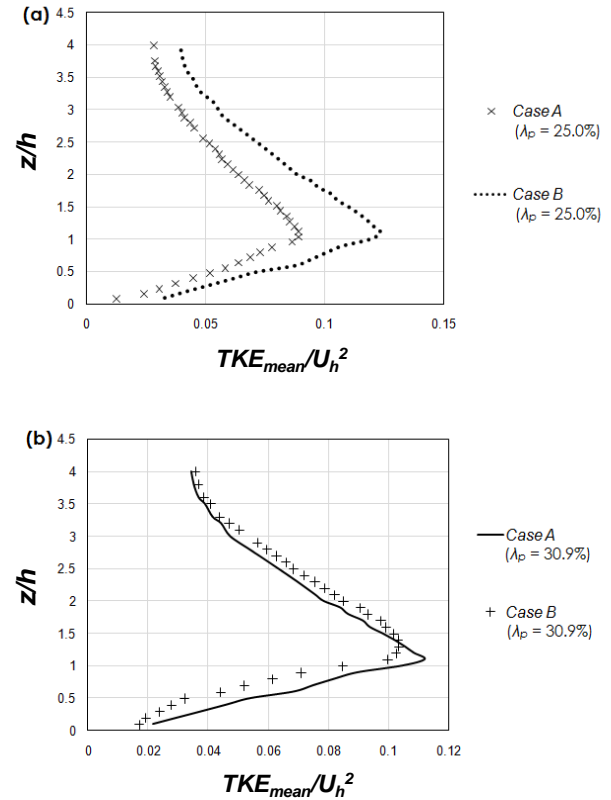


**Figure 8** Comparison of mean TKE profiles of cases A and B with (a)  $\lambda_p = 25.0\%$  and (b)  $\lambda_p = 30.9\%$

In Figure 8(a), mean TKE values for case B are higher than those for case A, especially at the top of the block region. This indicates that the small roughness of case B impacted the mean TKE distribution with 25% packing density. However, the TKE profiles for the two cases with 30.9% packing density in Figure 8(b) are closely aligned.

In Figure 9, the mean TKE profiles for case A are in sync for the two different packing densities below the block height, while the mean TKE profiles for case B deviate from one another in the canopy region. This might be due to flow interruption and increased turbulence by small-scale roughness. The impact of small-scale roughness on the mean TKE profiles is most apparent within the canopy region, in which mean TKE values are higher in case B than in case A.

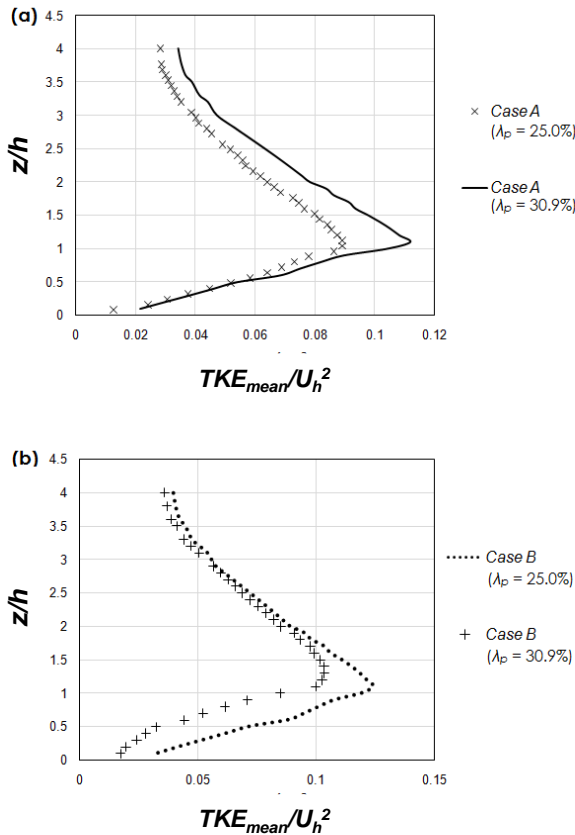


Figure 9 Comparison of mean TKE profiles for  $\lambda_p = 25.0\%$  and  $\lambda_p = 30.9\%$  for (a) case A and (b) case B

### 3.3 Drag Coefficient

Drag coefficient ( $C_d$ ) is a measure of the resistance or drag on a certain object in a fluid environment. It consists of a dimensionless shear surface stress term divided by the kinetic energy of fluid. Drag coefficient can be determined from the friction velocity,  $u^*$  [14]. Equation 3.1 shows the relationship between  $C_d$  and  $u^*$ :

$$u^* / U_{ref} = \sqrt{0.5C_d}, \quad (3)$$

where  $U_{ref}$  is the reference wind speed at the domain height.  $u^*$  can be obtained from the square root of the product of the pressure gradient and block height. From the data in Table 1, it can be deduced that the drag coefficient increases with  $\lambda_p$  [16, 17]. Mean velocity increases with greater  $\lambda_p$ , resulting in higher drag force. Additionally, increasing the small-scale roughness also affects the drag coefficient. Case B shows higher drag coefficient values than case A for the two packing densities. This finding is related to the higher TKE obtained for case A.

Table 1 Results of drag coefficient,  $C_d$

Case	Friction velocity, $u^*$ (m/s)	Reference velocity, $U_{ref}$ (m/s)	$C_d$
A ( $\lambda_p = 25.0\%$ )	<b>0.72</b>	<b>9.80</b>	<b>0.0107</b>
B ( $\lambda_p = 25.0\%$ )	<b>0.76</b>	<b>9.67</b>	<b>0.0123</b>
A ( $\lambda_p = 30.9\%$ )	<b>0.73</b>	<b>9.68</b>	<b>0.0114</b>
B ( $\lambda_p = 30.9\%$ )	<b>0.75</b>	<b>9.49</b>	<b>0.0125</b>

### 3.4 Flow Visualization

Figures 10 through 13 depict the flow visualisation below the canopy level. Wind vectors on the vertical  $xz$ -plane are plotted to visualise the left-right streamwise flow (along the  $x$ -axis). To focus on the flow below the height of the building (i.e. the canopy layer), the flow regimes were plotted from the ground level to two times the block height ( $2h$ ).

The gaps between blocks are  $1h$  for  $\lambda_p = 25.0\%$  and  $0.8h$  for  $\lambda_p = 30.9\%$ . In Figure 10 (for  $\lambda_p = 25.0\%$ ), a large recirculation flow appears behind the blocks, while in Figure 11 (for  $\lambda_p = 30.9\%$ ), this circulation flow still exists but is compressed by the gap. This pattern, known as skimming flow, is consistent with the results of other studies that investigated dense arrays of blocks [5, 18, 19].

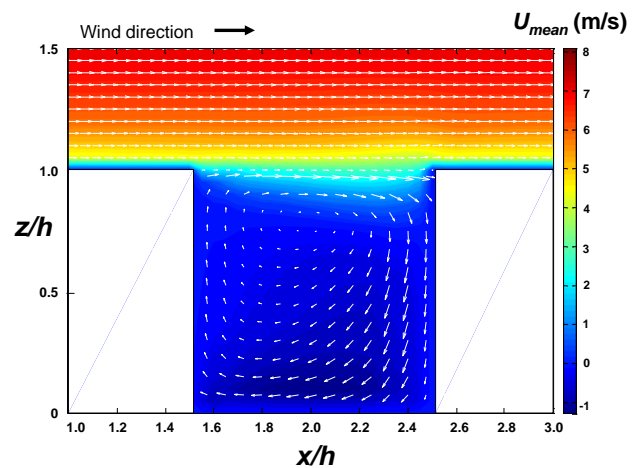
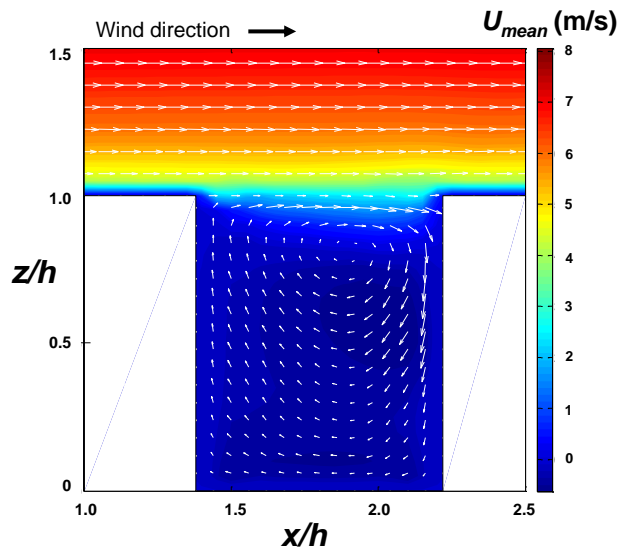
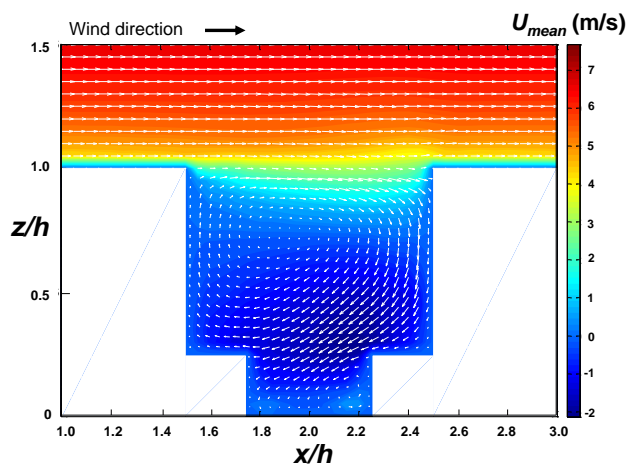


Figure 10 Mean flow structure for case A with  $\lambda_p = 25.0\%$  where white rectangular areas represent the buildings



**Figure 11** Mean flow structure for case A with  $\lambda_p = 30.9\%$  where white rectangular areas represent the buildings

In addition, differences in gaps between blocks and small roughness result in different flow patterns [2, 3], as shown in Figures 12 and 13. Both figures show a small vortex with a counter-rotational flow in the canyon region near the small-scale roughness element. The flow starts to split into two directions at the edge of the additional small roughness element. This separation generates another small vortex below the large recirculation flow.



**Figure 12** Mean flow structure for case B with  $\lambda_p = 25.0\%$  where white rectangular areas represent the buildings

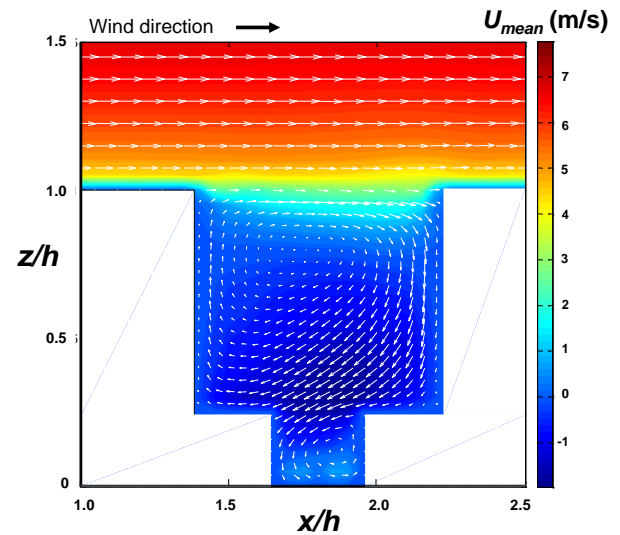


**Figure 13** Mean flow structure for case B with  $\lambda_p = 30.9\%$  where white rectangular areas represent the buildings

## 4.0 CONCLUSION

The comparison of wind flow characteristics between arrays of cubical blocks (case A) and cubical blocks with small-scale roughness (case B) was achieved using the computational fluid dynamics technique through RANS simulations with the RNG  $k-\epsilon$  model.

The validation results for the velocity profiles are consistent with the findings from previous research, thus supporting the reliability of this study. The results show that the streamwise velocity for case A was higher than that of case B, while TKE in case B was higher than in case A. These findings highlight the impacts of small-scale roughness on wind flow characteristics. The comparison between 25.0% and 30.9% packing densities shows some discrepancy, particularly in the TKE profiles. The impact of small-scale roughness on flow structures surrounding block arrays is substantiated by the flow vector visualisations for the streamwise direction.

The number of studies concerned with the effect of small-scale roughness is limited. This study is among the first to provide results for the comparison of wind flow characteristics between arrays of cubical blocks and cubical blocks with small-scale roughness elements. These findings can contribute to further research on wind behaviour, especially within the simplified urban environment.

## Acknowledgement

This research was financially supported by the Malaysian Ministry of Higher Education (MOHE) under the Fundamental Research Grant Scheme (Vot 4F598) and Research University Grant (Vot 10J91) of Universiti Teknologi Malaysia.

## References

- [1] Skote, M., and M. Sandberg. 2005. Numerical and Experimental Studies of Wind Environment in an Urban Morphology. *Atmospheric Environment*. 39(33): 6147-6158.
- [2] Oke, T. R. 1988. Street Design and Urban Canopy Layer Climate. *Energy and Buildings*. 11(1-3): 103-113.
- [3] Coceal, O., T. G. Thomas, I. P. Castro, and S. E. Belcher. 2006. Mean Flow and Turbulence Statistics over Groups of Urban-like Cubical Obstacles. *Boundary-Layer Meteorol.* 121: 491-519
- [4] Salizzoni, P., L. Soulhac, P. Mejean, and R. J. Perkins. 2008. Influence of a Two-Scale Roughness on a Neutral Turbulent Boundary Layer. *Boundary-Layer Meteorol.* 127: 97-110.
- [5] Saji, N. 2012. A Review of Malaysian Terraced House Design and the Tendency of Changing. *Journal of Sustainable Development*. 5(5): 140-149.
- [6] Sazally, S. H., E. O. Omar, H. Hamdan, and A. F. I. Bajunid. 2009. *Procedia - Social and Behavioral Sciences*. 49: 319-327.
- [7] Abd Razak, A., A. Hagishima, N. Ikegaya, and J. Tanimoto. 2013. Analysis of Airflow over Building Arrays for Assessment of Urban Wind Environment. *Building & Env.* 59: 56-65.
- [8] Mochizuki, S., and F. T. M. Nieuwstadt. 1996. Reynolds-Number-Dependence of the Maximum in the Streamwise Velocity Fluctuations in Wall Turbulence. *Exp. In Fluids*. 21: 218-226.
- [9] Xie, Z.-T., O. Coceal, and I. P. Castro. 2008. Large-Eddy Simulation of Flows over Random Urban-like Obstacles. *Boundary-Layer Meteorol.* 129: 1-23.
- [10] Mohammad, A. F., S. A. Zaki, M. S. M. Sukri, A. Hagishima, and A. Abd Razak. 2014. Large-Eddy Simulation of Wind-Induced Ventilation in Urban Buildings of Random Staggered Arrays. *Proceedings of Computational Wind Engineering 2014*, June 8-12. Hamburg, Germany.
- [11] Mohammad, A. F., S. A. Zaki, A. Hagishima, and M. S. M. Ali. 2014. Determination of Aerodynamic Parameters of Urban Surfaces: Methods and Results Revisited. *Theor. Appl. Climatology*. DOI: 10.1007/s00704-014-1323-8.
- [12] Zaki, S. A., A. Hagishima, J. Tanimoto, and N. Ikegaya. 2011. Aerodynamic Parameters of Urban Building Arrays with Random Geometries. *Boundary-Layer Meteorol.* 138: 99-120.
- [13] Cheng, Y., F. S. Lien, E. Yee, and R. Sinclair. 2003. A Comparison of Large Eddy Simulations with a Standard k-E Reynolds-Averaged Navier-Stokes model for the Prediction of a Fully Developed Turbulent Flow over a Matrix of Cubes. *Journal of W. Eng. and Ind. Aerodyn.* 91: 1301-1328.
- [14] Stull, R. B. 1988. *An introduction to Boundary Layer Meteorology*. Dordrecht: Kluwer Academic Publishers.
- [15] Hang, J., Y. Li, and M. Sandberg. 2011. Experimental and Numerical Studies of Flows through and within High-Rise Building Arrays and Their Link to Ventilation Strategy. *Journal of W. Eng. and Ind. Aerodyn.* 99: 1036-1055.
- [16] Hagishima, A., J. Tanimoto, K. Nagayama, and S. Meno. 2009. Aerodynamic Parameter of Regular Arrays of Rectangular Blocks with Various Geometries. *Boundary-Layer Meteorol.* 132: 315-337.
- [17] Zaki, S. A., A. Hagishima, J. Tanimoto, A. F. Mohammad, and A. Abd Razak. 2014. Estimation of Aerodynamic Parameters of Urban Building Arrays Using Wind Tunnel Measurements. *Journal of Eng. Science and Tech.* 9(2): 176-190.
- [18] Kanda, M., R. Moriwaki, and F. Kasamatsu. 2004. Large-Eddy Simulation of Turbulent Organized Structures within and above Explicitly Resolved Cube Arrays. *Boundary-Layer Meteorol.* 112(2): 343-368.
- [19] Kono, T., T. Tamura, and Y. Ashie. 2010. Numerical Investigation of Mean Winds within Canopies of Regularly Arrayed Cubical Buildings under Neutral Stability Conditions. *Boundary-Layer Meteorol.* 134: 131-155.